Research Article

The influence of bio-optical properties of *Emiliania huxleyi* and *Tetraselmis* sp. on biomass and lipid production when exposed to different light spectra and intensities of an adjustable LED array and standard light sources

Tim Granata[1] · **Patrick Habermacher**[2] · **Vinzenz Härri**[2] · **Marcel Egli**[1]

Abstract

The effects of bio-optical characteristics on lipid and biomass production rates for *Emiliania huxleyi* and *Tetraselmis* sp. were studied under different irradiances and spectra. Biomass and lipid production increased from irradiances of 50–800 µE m^{-2} s^{-1} but differed for each spectrum. The highest biomass and neutral lipid production rates for *E. huxleyi* occurred under a red-blue LED array, which mimicked the absorption spectra of the cell's chlorophyll *a* and accessory pigments, especially fucoxanthins. Biomass and neutral lipid production for *Tetraselmis* sp. were enhanced under broader spectra of cool white and grow lights. Neutral lipids per cell volume were similar for the two species and inversely proportional to chlorophyll *a* concentrations. High biomass and neutral lipid production rates were associated with high total quantum absorption and low quantum absorption per cell. Generally, quantum efficiencies were highest for high light treatments with high total quantum absorption and high production rates. Using reconstructed quantum absorption by pigments, the bio-optical model showed that photoprotective pigments were dependent on light intensity and spectra. Quantum efficiencies increased when excluding the contribution of photoprotective pigments to total quantum absorption since they did not directly contribute to photosynthesis, but did promote higher production rates.

Electronic supplementary material The online version of this article (https://doi.org/10.1007/s42452-019-0529-x) contains supplementary material, which is available to authorized users.

✉ Tim Granata, timothy.granata@hslu.ch; Patrick Habermacher, patrick.habermacher@hslu.ch; Vinzenz Härri, vinzenz.haerri@hslu.ch; Marcel Egli, marcel.egli@hslu.ch | [1]Bioscience and Medical Technology, Lucerne University of Applied Science and Art, (Hochschule Luzern), Obermatt 9, 6052 Hergiswil, Switzerland. [2]IIES, Lucerne University of Applied Science and Art, Lucerne (Hochschule Luzern), Technikumstrasse 21, 6048 Horw, Switzerland.

SN Applied Sciences (2019) 1:524 | https://doi.org/10.1007/s42452-019-0529-x

Received: 22 December 2018 / Accepted: 26 April 2019

Published online: 06 May 2019

Graphical abstract

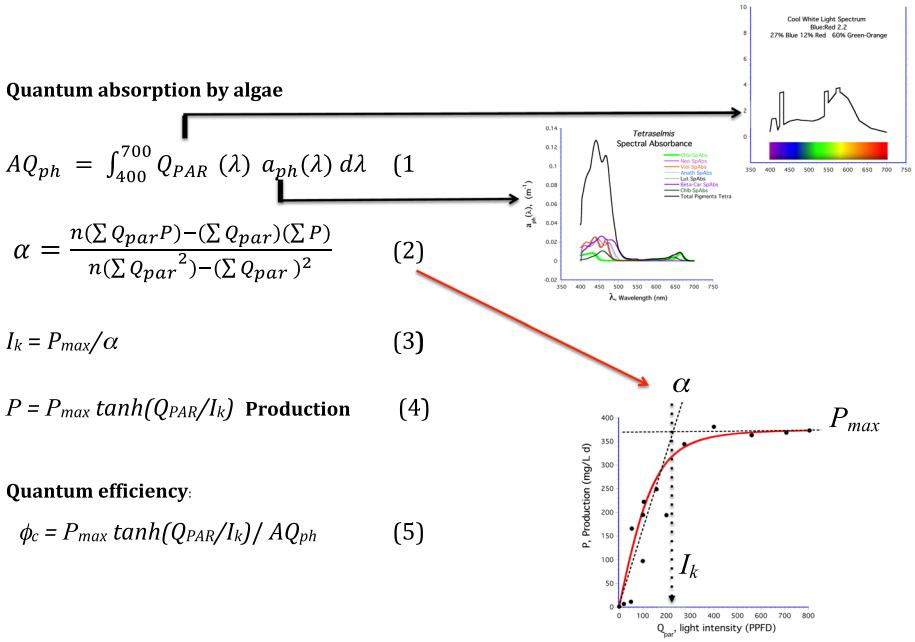

Keywords Bio-optical properties · Spectral irradiance · Biomass and lipid production

Mathematics Subject Classification 92C99

JEL Classification Q42

Abbreviations

NPQ	Non-photochemical quenching
PAR	Photosynthetically active radiation
PPFD	Photosynthetic photon flux density
PPP	Photoprotective pigments
PSP	Photosynthetic pigments
PSI	Photosystem I
PSII	Photosystem II

1 Introduction

Bio-optics of marine and freshwater phytoplankton have been well studied for spectral properties by aquatic ecologists [1–5], but few studies in the algal biofuel community have measured spectral characteristics of microalgae, e.g., Kandilian [6]. Yet bio-optics are important since the rate of photosynthesis depends on photon capture by algal cells. This rate can be parameterized for absorption of light by cell pigments and thus is directly regulated to biomass production [7] and efficiency [3].

Bio-optics are most pertinent to biofuel production where large cultures with relatively dense cell concentrations attenuate irradiance as a result of photon absorption by culture medium and by algal pigments. In the outer surface of the mass cultures, where light intensity is high, algae slowly decrease their antenna size (< 12 h) providing the timescales of mixing are sufficient [8]. A smaller antenna size is a result of a reduction in total chlorophyll and accessory pigment concentrations associated with the light reaction centers of photosystems I and II (PSI and PSII). The smaller antenna size causes cells to saturate at higher light intensities with higher biomass production rates [9].

The opposite happens to cells near the bottom of raceways and in the interiors of closed photoreactors. These cells acclimate to low light by producing more pigments relative to their reaction centers, thereby increasing their antenna size. A larger antenna allows cells to saturate at lower light intensities producing biomass at higher quantum efficiency. However, when these low light acclimated cells circulate into high light, they tend to photoinhibit on a very short timescale (seconds to minutes) as excess photon energy reduces photosynthesis and ultimately biomass production. Reduced production has been one of the major problems in mass cultures since cells are exposed to a high irradiance on the surface, but a low photosynthetic

photon flux density (PPFD) deeper in the culture. Attenuation of light affects not only the quantum flux of photons but also their spectral distribution. The culture medium absorbs red wavelengths more than blue [10]; however, the spectral absorption by algae depends on the concentration of various pigments in their reaction centers and antenna [1].

Mutants were developed with smaller antenna sizes that efficiently used photons, enhancing productivities per pigment concentration over those of wild types containing more accessory pigments and reaction centers. Although production per antenna size improved using mutants, the production per cell remained about the same as [11–13] or lower than the wild types [14]. A more recent approach reduced the concentration of chlorophyll *b* per cell, thereby reducing the antenna size by approximately 50% [15]. While this about doubled production per unit chlorophyll, production per cell was about the same as the wild type.

Another way to achieve higher production rates is to select algal species that: (1) acclimate to high light without severe photoinhibition; (2) have small antenna sizes; and (3) can achieve high production rates. The coccolithophore *Emiliania huxleyi* can acclimate to high light environments and has high productivity [16], which recent investigations suggest are linked to the cell's ability to adjust concentrations of accessory pigments [17, 18].

The spectral composition of light has been shown to interact with the spectral properties of accessory pigments to affect biomass production rate [18]. Different blue light spectra were found to give higher rates of primary production than white light for *E. huxleyi* [19] and the coccolithophore *Isochrysis* [20]. In contrast, green algae had enhanced production in red light compared to white and green lights [21]. Lipid production for green algae has been shown to be higher in blue light than in white [22], red [23], yellow, green, or purple light [24]. For the cyanobacteria *Spirulina,* growth in blue light was inferior to red, yellow, green, and white lights [25, 26], which might be expected since these cells possess phycobiliprotein pigments in their antenna that absorb light in longer wavelengths (500–650 nm). However, few of these studies measured the specific absorption or analyzed the bio-optical properties of the cells under these spectrally different light regimes.

In this study, we contrast the bio-optical properties of *E. huxleyi*, which does not readily photoinhibit, to those of the green algae *Tetraselmis* sp., a species used for many biofuel studies [27–31]. Both species produce a suite of photosynthetic pigments (PSP) and photoprotective pigments (PPP) that can exploit different wavelengths in the visible light spectrum. To determine how cells react to different light spectra, treatments were exposed to commercially available light sources and a novel light emitted diode (LED) array with different spectral peaks. Unlike studies that used only narrow band, monochromatic wavelengths, the light sources used here are broader band and therefore more finely tuned to the absorption spectra for antenna pigments. The differences in production rates and optical properties of the two species were parameterized in a bio-optical model and analyzed to determine how quantum efficiencies of biomass and lipid production were dependent on light intensities and spectra.

2 Methods

2.1 Experimental treatments

Parent cultures of *E. huxleyi* (No. 1210) and *Tetraselmis* sp. (No. 2604) were purchased from the Roscoff culture collection and grown at a photosynthetic photon flux

Table 1 Spectral characteristics of light sources arranged by increasing percent of blue wavelengths

Light sources	Blue 440–505 nm	% Red 650–680 nm	% Blue–Green–Yellow 505–650 nm	Power demand *W*	Comments
Sun[1], noon cloudless	37	15	48	–	NOAA, lower atmosphere
Cool white	28	6	66	1140[3]	Company specification
GloPlus	44	11	45	170[4]	Company specification
LED RRBBB[2]	77	17	6	21.3	This study
LED RBBB[1]	87	9	4	21.3	This study
LED BBB[1]	100	0	0	21.3	This study

[1]Sun irradiance is spectrally close to GloPlus and cool white light used in this study

[2]BBB, RBBB, and RRBBB indicated array had 0, 1, and 2 red diode strings plus 3 blue

[3]1500 W based on 40 W per fluorescent bulb plus 20 W per ballast. In all 25 of each are needed for 800 PPFD

[4]272 W based on 24 W per GloPlus bulb + 10 W per ballast. Eight bulbs and ballasts are needed for 800 PPFD

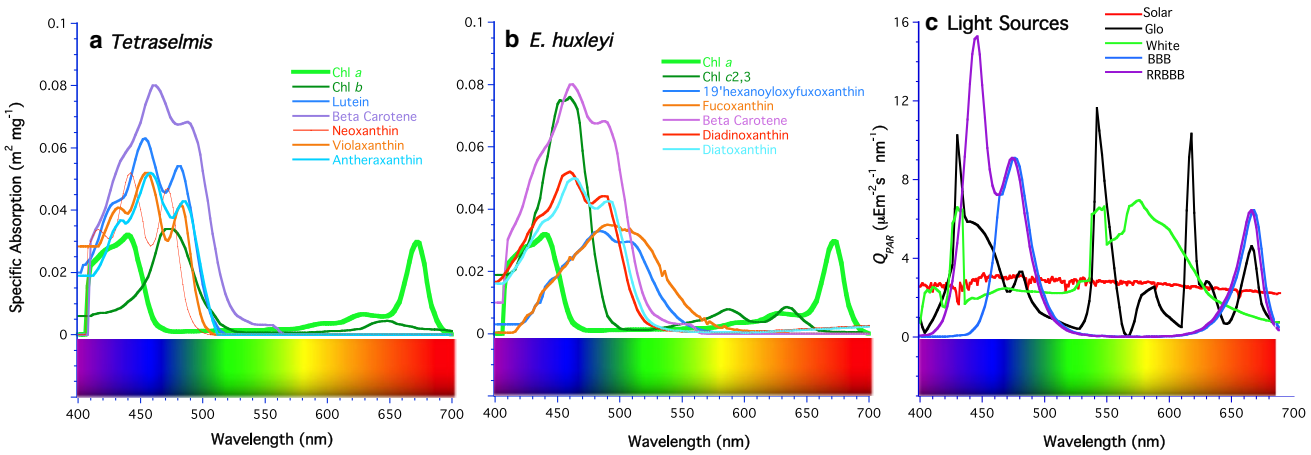

Fig. 1 Spectra of specific absorption (m^2 mg^{-1}) for: **a** *Tetraselmis* sp. pigments and **b** *E. huxleyi* pigments. **c** Spectral irradiance of sunlight compared to the light sources used in this study: GloPlus light, cool white light, and LEDs configured for high red and blue (RRBBB), low red and high blue (RBBB), and blue only (BBB). Solar spectral irradiance is only shown as a reference to light sources but was not used in this study. All irradiances were scaled to an integral PAR value of 800 μE m^{-2} s^{-1}. The peaks in cool white and GloPlus lights are due to the mercury arc of the bulbs. The color scale bar shows the relationship to the quantum visible spectrum

density (PPFD) of 200 μE m^{-2} s^{-1} on a 14:10 light/dark cycle using GloPlus grow bulbs (Hagen T8). Cells were maintained on either on *f*/2 (*E. huxleyi*) or *h*/2 (*Tetraselmis* sp.) growth medium [32] at a salinity of 33 ppt in artificial seawater (Instant Ocean) [33] and the pH adjusted to 8.3 with 2000 μM Na_2CO_3. Treatments were run in duplicate in T-flasks (70 ml), inoculated with parent cultures, and filled with media to eliminate headspace. Parent cultures and experimental treatments were maintained in a cold room at 15 ± 1.5 °C.

Treatments were maintained as semi-continuous cultures by halving the volume every 7 days, while the cells were in the exponential growth phase, allowing cells to photoacclimate to the light conditions listed in Table 1. After treatments were photoacclimated, they were diluted to the same concentration and the experiments conducted over a 7-day period. Five different light sources with different spectra were studied: (1) grow lights (Glo); (2) white light (W); (3) blue LEDs (BBB); (4) BBB LEDs with low red (RBBB); and (5) BBB LEDs with high red (RRBBB). The light sources were fluorescent cool white light (Osram 940), fluorescent GloPlus light (Glo), and a variable spectrum, LED array. Spectra for the light sources and for algal absorption are shown in Fig. 1.

The LED array was adjustable to three different spectra: three blue diode strings for a blue light spectrum (BBB), one red and three blue diodes strings for a blue and low red spectrum (RBBB), and two red and three blue strings (RRBBB). The RBBB and RRBBB spectra were tuned to match the absorption spectrum for chlorophylls and accessory pigments of *E. huxleyi,* and, to some extent, of *Tetraselmis* sp.

The GloPlus (grow light, Glo) has peak emissions in the blue, green, and yellow-red bands. Cool white light had a narrow peak in the blue, broader peaks in green to yellow bands, and a temperature rating of 4100 K, which is close to the color of solar irradiance of 5100 K. In comparison with these light sources, solar irradiance is relatively flat with a slight decrease from blue to red wavelengths. Overall, percent blue was higher for the LED array than for other light sources, which complemented the algal absorption spectra for these two species (Table 1).

Treatments were maintained at nominal irradiances of 0, 50, 100, 200, 400 and 800 μE m^{-2} s^{-1} (photosynthetic photon flux density, PPFD) to determine production–irradiance (*P* – *I*) curves for each spectrum. These represent a range from undersaturated (0–100 PPFD) to near or saturated (200–800 PPDF) intensities. Light intensity was measured as photosynthetically active radiation (Q_{PAR}) using a Apogee quantum meter, which integrated visible wavelengths from 400 to 700 nm. Daily cell counts were done on a Zeiss light microscope, and specific growth rate was calculated as $\mu = ln(N_2/N_1)/(t_2 - t_1)$ where N_t corresponds to cell number at times t_2 and t_1.

For treatments at 800, 400, 200, and 50 PFFD, neutral lipid content per cell was determined by staining cells with BODIPY [31] and measuring fluorescence at 533 nm on the flow cytometer (BD Accura C6), which, like Nile Red, gives a florescent signal proportional to the mass of neutral lipids [34]. No correction was made to the neutral lipid fluorescence since the background for unstained cells was 10^3 orders of magnitude lower. Simultaneously, chlorophyll *a* fluorescence per cell at 675 nm, cell concentration, and forward scatter were also determined using the flow

cytometer. Neutral lipid fluorescence was plotted against chlorophyll *a* fluorescence and cells gated to ensure only algal cells were sampled. Forward scatter height was calibrated to seven sizes of polystyrene microbeads with diameters from 2 to 15 µm (Spherotech Inc).

At the end of each experiment, one of the replicates was dried to determine biomass, and the second replicate was extracted for pigments. For dry weight biomass, treatment volumes of 60 ml were filtered onto pre-dried, pre-weighted GF/C filters using a Millipore filter apparatus and vacuum pump (45 mm Hg). Filtered cells were washed 3 times with DI water to remove salts and each time the vacuum was disconnected so cell would not be damaged. Filters were then dried at 105 °C for 2 h and cooled in a desiccator until a constant weight was attained. The dried biomass was also used to determine neutral lipids as FAMEs, by first freezing filters at − 20 °C, solubilizing biomass in 0.2 ml chloroform/methanol (2:1 v/v) and immediately adding 0.3 ml methylated HCL (Sigma) to complete transesterification [35]. However, the FAME procedure did not give consistent results for standards and samples, even though the water content was 0%. Consequently, neutral lipids are only presented as a relative fluorescence per cell. Fluorescent microscopic images of stained cells showed that neutral lipids were present in lipid bodies.

Pigments were extracted from a sample volume of 50 ml that was filtered onto GF/C at 0.5 atm with 4 drops of $MgCO_3$ added to de-acidify the filters. Filters were placed in 15-ml Falcon tubes with 6 ml of 90% ethanol, vortexed for 5 s, then placed in ultrasonic cold water bath (35 kHz) for 15 min. Pigments were left to extract in the dark overnight in a 5 °C refrigerator, after which 1.5 ml of the well mixed extract was transferred to HPLC vials and immediately processed following the SCOR-UNESCO [36] protocol. Pigments were analyzed on a HPLC Pump PU 2089plus (Jasco System) equipped with an AS2055Plus Autosampler, $CO_2$060Plus column oven, and a MD 2018Plus diode array detector with a resolution from 300 to 900 nm. The column was a stationary phase C18 column (Merck, LiChrospher 100 RP-18/5 µm/250-4). The column temperature was maintained at 30 °C. The starting eluent was 35.0% methanol, 45.0% ethyl acetate, and 20.0% deionized water; the final effluent was 55.0% methanol, 45.0% ethyl acetate, 0% water. The flow rate was 1 ml min^{-1} and the run time 35 min per sample. Spectral information was consistent with a library of chlorophyll and carotenoid spectra. Pigments were calibrated to standards from DHI (Denmark). The spectral distribution of each pigment, from 400 to 700 nm, was determined by normalizing its spectral area to 1.0 and multiplying the pigment concentration (mg m^{-3}). Pigment absorption, a_i (λ), was calculated by multiplying the weight-specific absorption of each pigment (Fig. 1a, b) by the normalized spectral pigment distribution [2, 37].

2.2 The light emitting diode (LED) array

The LED array was designed and built at the Lucerne University of Applied Science and Arts to match the absorption chlorophyll *a* spectra of *E. huxleyi* and *Tetraselmis* sp. with peaks in the red and blue wavelengths [38]. The LED array had to meet not only the spectral requirements, but also requirements for irradiance intensity, energy consumption, and heat emission, to ensure the successful cultivation of the algae.

The irradiance intensity requirements were 0–1600 µE m^{-2} s^{-1} (0–391 Wm^{-2}) for an array with a small, 0.03 m^2, footprint (20 cm × 15 cm). The power of the array was calculated as 36 W (3 × 391 Wm^{-2} × 0.03 m^2), where the factor 3 accounted for 1/3 of the irradiance at a distance of 10 cm from the array. The online tool *Phillips Lumileds* was used to specify the number and type of LED diodes for a nominal current of 500 mA. Using the tool *LED Spectrum Mixer*, which mixes light of different LEDs with given luminous flux to determine the radiated power, the radiated power was iterated to give the luminous flux of the respective waveband. Given the emission of the single LED and the overall emission for each waveband, it was possible to calculate the required type of LED. Based on the algal action spectra (Fig. 1a, b), the blue peak was specified between 420 and 490 nm; therefore, two LED diodes were necessary, blue and royal blue, which accounted for 40% of the radiated power. For the smaller red peak at 670 nm, a deep red LED diode was ideal and accounted for 20% of the radiated power.

The exact color composition was a mix of the three-color diodes, blue, royal blue, and deep red, in a energy ratio of 2:2:1. To meet the specified spectrum and irradiance level at the calculated power output, the array required 20 blue, 20 royal blue, and 10 deep red diodes for a total of 50 LEDs. The 50 LEDs were arranged in 5 strings (rows), 2 red/blue, and 3 blue. Each string could be controlled to reduce the PPFD for any combination of red and blue light. By adjusting the dash pods for spectral quality and the wattage to maintain constant irradiance, light treatments were produced for blue light (3 BBB strings), low red with blue (RBBB strings), and equal red and blue (RRBBB strings).

The final design requirement was to reduce the waste heat given off by the LED array, which was important for two reasons: (1) to prevent algae from being heated by the array so that cultures could be kept at the optimum temperature for growth and (2) to achieve the rated irradiance produced by the LEDs, which is extremely reduced at high operating temperatures. To achieve these criteria, diodes rather than resistors were used, drastically reducing thermal resistance of the board. An aluminum heat dissipater was mounted to the circuit board as a heat sink.

The heat dissipater had a thermal resistance of 0.08 K W^{-1}, and its maximum temperature was calculated assuming an ambient temperature of 15 °C and maximum power dissipation for 50 LEDs at 69.5 W (40 × 2.95 V × 0.5 A and 10 × 2.1 V × 0.5 A). The thermal resistance of the thermally conducting tape was 0.01 K W^{-1}, giving a maximum heat dissipater temperature of 21.3 °C (15 °C + [0.01 K W^{-1} + 0.0 8 K W^{-1}] × 69.5 W). Using the casing temperature, as well as the thermal resistance of the array, both of which influenced the heating loss of the LEDs, the temperature of the LEDs was calculated. The red LED dissipation loss was 1.5 W and 8 K W^{-1}, giving a maximum operating temperature of 29.7 °C (21.3 K W^{-1} + [1.05 W × 8 K W^{-1}]). The blue LED loss was 1.45 W and 10 K W^{-1}, resulting in a maximum operating temperature of 35.8 °C (21.3 K/W + [1.45 W × 1 0 K W^{-1})]. However, the array was never operated at maximum irradiance, so these temperature maxima were not reached. When the array was tested in a 15 ± 1.5 °C cold room at irradiances from 200 to 1600 µE m^{-2} s^{-1}, the temperature in 60-ml cultures at a distance of 10 cm from the array was elevated < 0.5 °C.

2.3 Bio-optical model

To compare the effects of light spectra on biomass and lipid production for each light intensity, the bio-optical spectral model of Bidigare et al. [3] was used, where the integrated, total quanta absorbed by algae for each light source was defined as:

$$AQ_{ph} = \int_{400}^{700} Q_{\mathrm{PAR}}(\lambda) a_{ph}(\lambda) \mathrm{d}\lambda \tag{1}$$

Spectral irradiance, Q_{PAR} (λ), for each light source and intensity was interpolated to 2 nm bins. Spectral algal absorption, a_{ph} (λ), was measured in visible wavelengths from 400 to 700 nm and resolved to 1 nm on a Cary 100 scanning spectrophotometer. The cuvette path length was 1 cm, and a blank consisting of the medium (i.e. *f*/2 or *h*/2), was subtracted from algal absorption. Absorption spectra were also reconstructed from HPLC analyses by summing the specific pigment absorbance multiplied by the pigment concentration [2]:

$$a_{ph}(\lambda) = \sum_{i}^{n} a_i(\lambda) C_i \tag{2}$$

To access quantum absorption of the different pigment groups, the carotene pigments containing oxygen (also called xanthophylls) were grouped, either as photoprotective pigments (PPP) or photosynthetic pigments (PSP). The xanthophylls antheraxanthin and beta carotene in *Tetraselmis* sp. are efficient at quenching fluorescence [39] and hence were grouped as PPP. The xanthophylls lutein, neoxanthin, and violaxanthin all contribute to photosynthesis in *Tetraselmis* sp. and were grouped with the chlorophyll pigments as PSP. The PPP xanthophylls in *E. huxleyi* were beta carotene and diatoxanthin, while PSP were chlorophylls, fucoxanthins, and diadinoxanthin. AQ_{PSP} and AQ_{PPP} represent the quantum absorption by PSP and PPP, respectively, and were calculated by substituting a_{PSP} and a_{PPP} for a_{ph}, in Eq. 1.

Biomass production was defined as $P_B = B\mu$, and production data were fitted to the Platt–Jassby model [40]:

$$P_B = P_{\max} \tanh\left(\frac{Q_{\mathrm{PAR}}}{I_k}\right) \tag{3}$$

where $P_{\max}$ is the maximum production based on the $P-I$ curve, α is the light-limiting photosynthetic rate measured as the initial slope of a linear regression of the $P-I$ curve, and I_k is the half-saturating constant of light determined as $P_{\max}\,\alpha^{-1}$.

Quantum efficiency of biomass and neutral lipid production of *E. huxleyi* and *Tetraselmis* sp. for different light sources and irradiances was parameterized following Bidigare et al. [3] as:

$$\phi_B = \frac{P_{\max} \tanh\left(\frac{Q_{\mathrm{PAR}}}{I_k}\right)}{AQ_{ph}} \tag{4}$$

ϕ_B is proportional to moles carbon fixed per Einstein (moles *C Ein*$^{-1}$). Similarly, the efficiency of neutral lipid production was defined as:

$$\phi_{\mathrm{NL}} = \frac{(\mathrm{NL})P_{\max} \tanh\left(\frac{Q_{\mathrm{PAR}}}{I_k}\right)}{AQ_{ph}} \tag{5}$$

where NL is neutral lipid fluorescence per cell, standardized by the maximum fluorescence to give a relative efficiency.

2.4 Statistical procedures

Linear and nonlinear regressions were preformed using Synergy Software (KaleidaGraph v4.5.3). Analysis of Variance (ANOVA), Chi-squared tests, Tukey's tests, and Student's t tests were performed at α = 0.05 or 0.001 significance levels using SPSS v25 software. Chi-squared tests were used to determine normality of distributions. ANOVA data were grouped into species (2), light intensities (3), and light sources (4) with replicates for each treatment to determine overall differences within and among variables. Post hoc Tukey's tests discriminated which groups differed. For each species, mean and standard deviations for

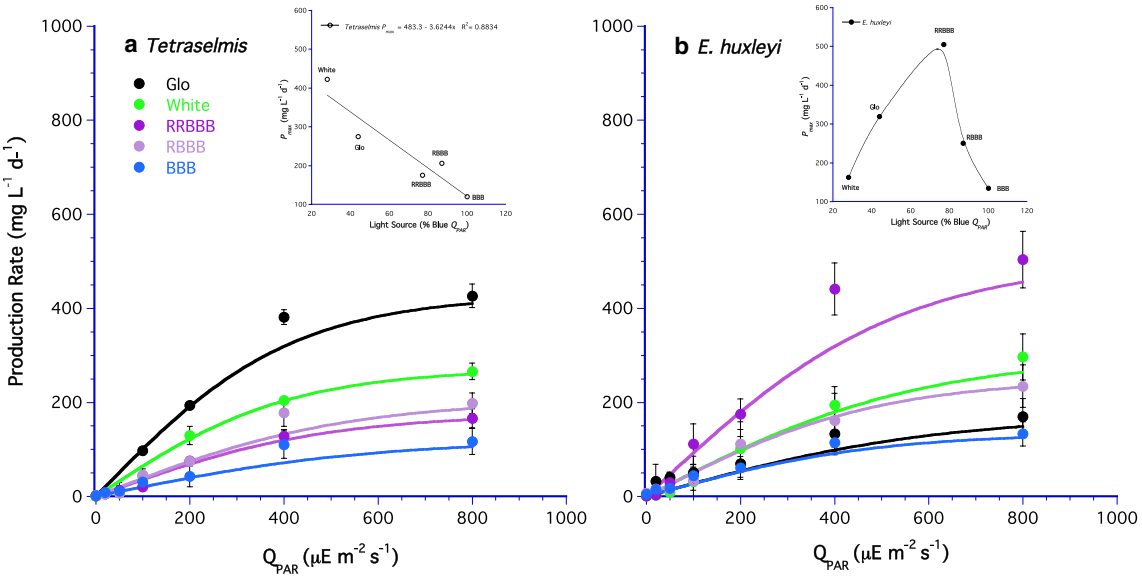

Fig. 2 Biomass production versus Q_{PAR} irradiance. **a** *Tetraselmis* sp. and **b** *E. huxleyi*. Curve fit to biomass is the hyperbolic tangent model of Platt and Jassby [40]. The inset for each species shows the maximum production rate as a function of the percent blue light from each light source. Means ± 2 standard deviations ($N = 2$)

production rates, cell counts, chlorophyll *a* fluorescence, and neutral lipid fluorescence were calculated from two replicate samples for each treatment. For each replicate, flow cytometer measurements of cell size, neutral lipid fluorescence, and chlorophyll *a* fluorescence were based on 10^4 cell counts. At the end of the experiment, one replicate was filtered for dry weight and lipid analysis and the second replicate was used for HPLC analysis of pigments. Thus, pigment data from extracts were based solely on unreplicated treatments. Replicate treatments of chlorophyll *a* fluorescence measurements, however, had low variability; therefore, it was assumed the extracted pigments were representative of the treatments. Additionally, for ANOVAs, the pooled treatment groups of extracted pigments increased the N and degrees of freedom for comparisons of light intensity and spectra.

Table 2 Parameters for bio-optical model of reconstructed cell absorption

	P_{max} mg L^{-1} d^{-1}	Intercept, b^1	Slope, α^1 (mg L^{-1} d^{-1}) (µ E m^{-2} s^{-1})$^{-1}$	R value^2	I_k µE m^{-2} s^{-1}	P^3_{error} σ^2
Tetraselmis sp.						
Glo	428 (25.0)	18.8	1.03	0.96	416	0.30
White	271 (17.4)	−9.33	0.66	0.95	410	0.84
BBB	120 (28.0)	7.77	0.21	0.95	579	0.35
RRBBB	176 (20.5)	−5.62	0.36	0.94	482	1.8
E. huxleyi						
Glo	173 (38.0)	−14	0.28	0.83	616	4.6
White	300 (49.1)	−11.6	0.52	0.95	578	1.0
BBB	135 (26.0)	3.88	0.28	0.95	482	1.6
RRBBB	505 (60.1)	−3.68	0.94	0.96	537	0.14

Mean P_{max} (standard deviations, $N = 2$)

[1]Linear regressions of $P-I$ curves. $P = b + \alpha Q_{PAR}$ for $0 \le Q_{PAR} \le 200$ µE m^{-2} s^{-1} to determine α and I_k

[2]Regression coefficients for linear fits of α, where $p < 0.0001$ for all treatments except *E. huxleyi* Glo, where $p = 0.001$

[3]Residual error: $P-I$ curve minus measured biomass production as variance over Q_{PAR}

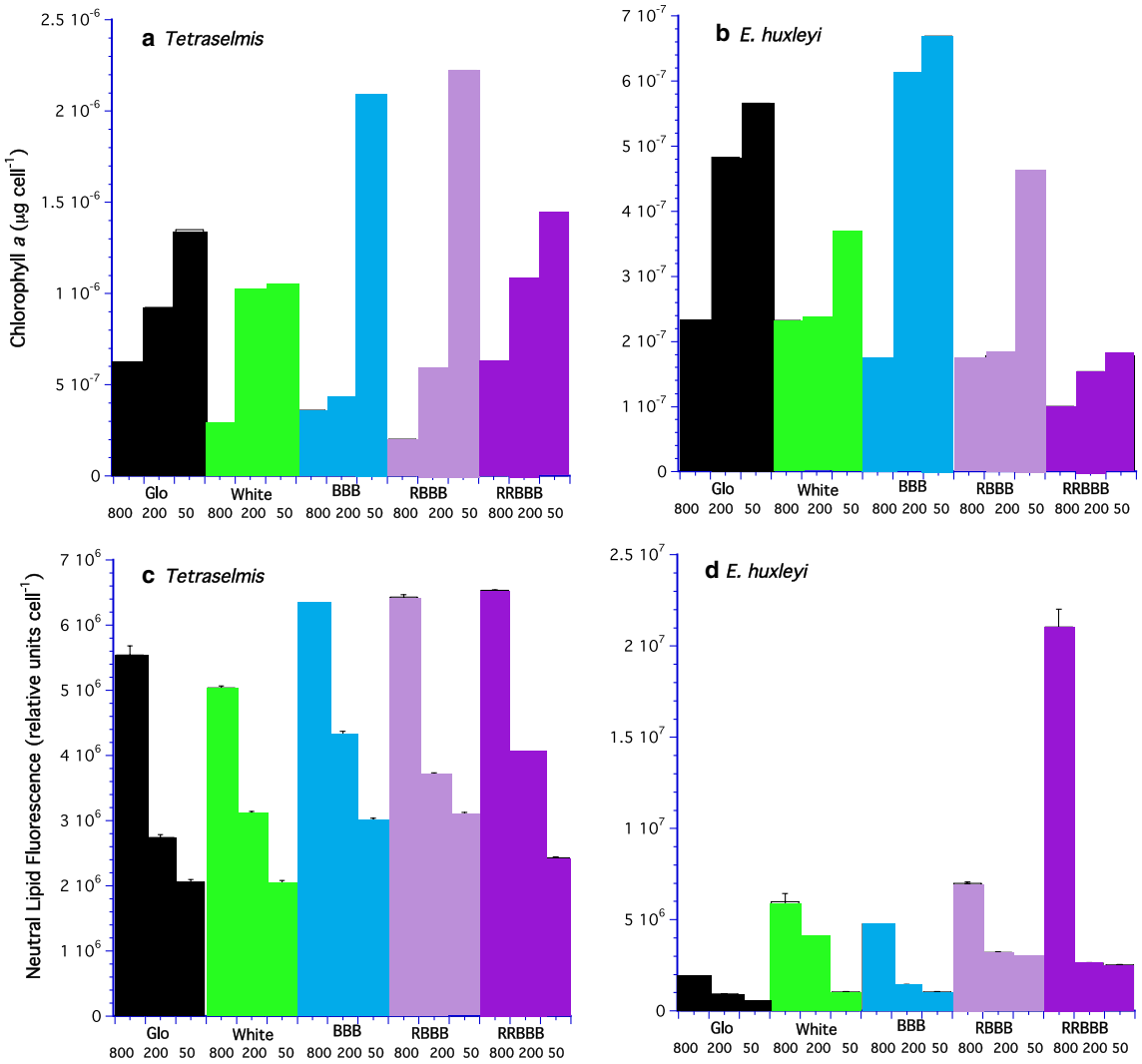

Fig. 3 Chlorophyll *a* concentration per cell and neutral lipid fluorescence per cell for 3 irradiances. **a** *Tetraselmis* sp. chlorophyll *a*, **b** *E. huxleyi* chlorophyll *a*, **c** *Tetraselmis* sp. neutral lipids, and **d** *E. huxleyi* neutral lipids. Means ± 2 standard deviations ($N = 2$). Colors same as Fig. 2

3 Results

3.1 Biomass production

Biomass production for both species was highly dependent on the intensity of the light source and its spectral composition, which was characterized by the percent blue, red, and blue-green-yellow wavebands (see Table 1). The highest biomass production rates for both species were at 800 PPFD (Fig. 2a, b), with *E. huxleyi* achieving over 500 mg L^{-1} d^{-1}, and *Tetraselmis* sp. just over 400 mg L^{-1} d^{-1}. Maximum production rates of *Tetraselmis* sp. for the 5 light sources decreased linearly with the percent of blue light with BBB < RRBBB < RBBB < Glo < white (Fig. 2a insert). P_{max} was also directly correlated with the percent of blue-green-yellow light, but had no correlation to percent red light (Supplement 1a). The maximum biomass production for *E. huxleyi* was highly nonlinearly related to the light source with BBB < white < RBBB < Glo < RRBBB (Fig. 2b insert). However, P_{max} was directly correlated with the percent of red light (Supplement 1b). Generally, *Tetraselmis* sp. production rates were linear until about 200 PPFD, indicating cells were light saturated at irradiances ≥ 200 PPFD. In contrast, most production rates for *E. huxleyi* were only saturated at higher light levels (≥ 400 PPFD).

Parameters for the bio-optical model derived from the $P-I$ curves showed that BBB treatments had the lowest α values for both species (Table 2). Glo and white light gave the highest α values for *Tetraselmis* sp. compared to RRBBB for *E. huxleyi*. The average α values for *Tetraselmis* sp. decreased with the percent of blue light (Supplement 2a), reflecting the same trend as P_{max} (Fig. 2a insert), though this is not surprising since α is directly proportional to P_{max} and inversely related to I_k. Similarly, α values for *E. huxleyi*

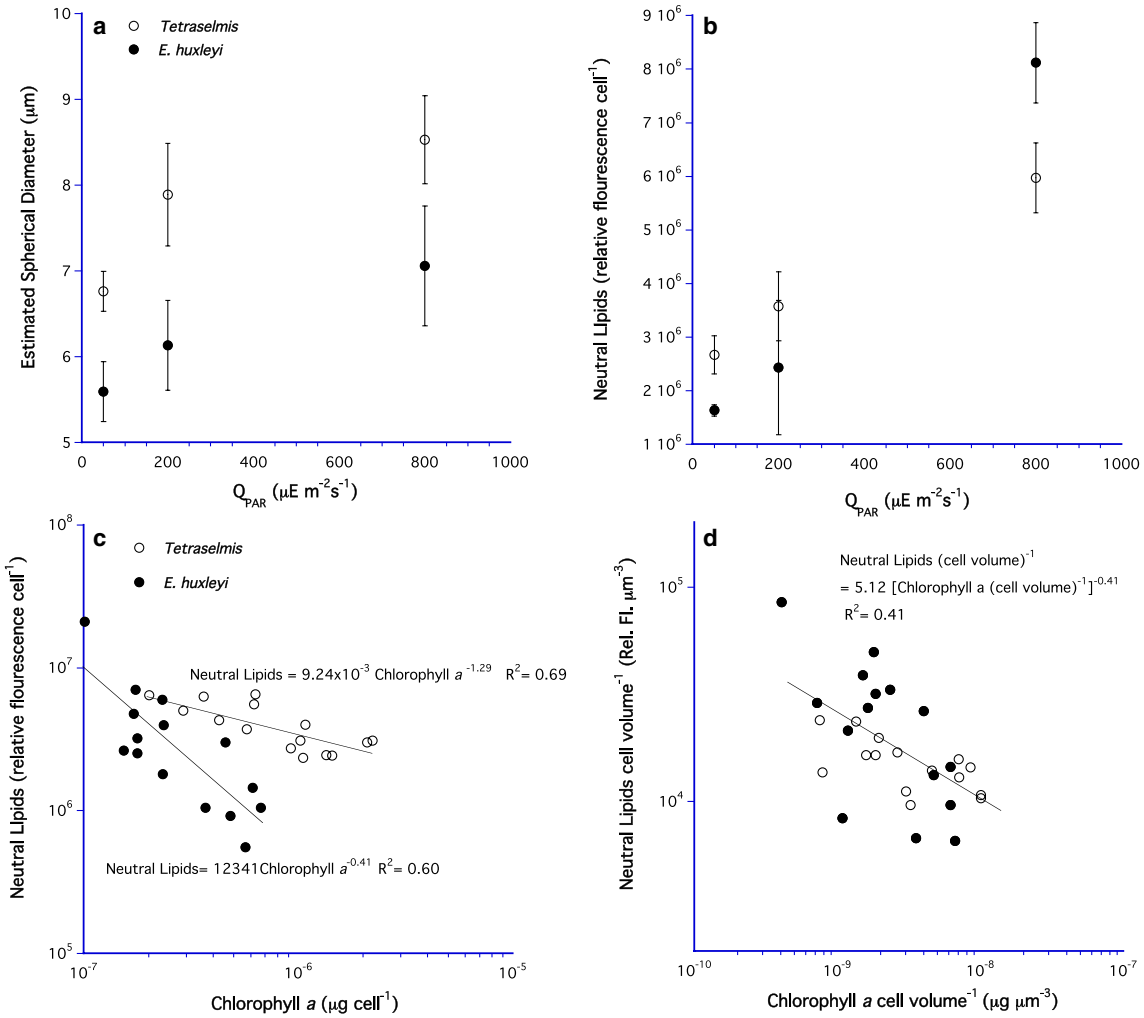

Fig. 4 Average cell size as a function of Q_{PAR} irradiance for: **a** *Tetraselmis* sp. and *E. huxleyi*. Neutral lipid fluorescence per cell as a function of: **b** Q_{PAR} and **c** chlorophyll *a* concentration per cell; and **d** neutral lipid fluorescence per cell volume versus chlorophyll *a* concentration per cell volume. Means ± 2 standard deviations ($N = 2$)

followed the same nonlinear trend as P_{max} (Supplement 2a). The average I_k for *Tetraselmis* sp. (482 PPFD) was lower than for *E. huxleyi* (540 PPFD).

3.2 Pigments, neutral lipids, and cell size

Chlorophyll *a* concentrations per cell for *Tetraselmis* sp. were twice as high as *E. huxleyi* concentrations (Fig. 3a, b). For both species, there was a negative trend between chlorophyll and irradiance. Chlorophyll *a* per cell decreased with increasing irradiance, although there was variability for the 200 PPFD treatments (Fig. 3a, b). The opposite trend was found for lipid fluorescence per cell, which increased with increasing irradiance (Fig. 3c, d).

Cell diameters increased with increasing irradiance (Fig. 4a) for both *Tetraselmis* sp. ($df = 14$, $F = 17.804$, $p < 0.001$) and *E. huxleyi* ($df = 11$, $F = 15.729$, $p = 0.001$), which was not a result of growth cycles since the growth phase was synchronized by the light/dark cycle. Only *E. huxleyi* under BBB light had the same diameters at all irradiances. No size dependence was found for spectral irradiance. The maximum volume for *E. huxleyi* was 247 $μm^3$ compared to the larger *Tetraselmis* sp. cells, which had a volume of 397 $μm^3$. Neutral lipid fluorescence also increased with cell size (Fig. 4b). Müller et al. [41] showed cell size decreased with light and nitrate limitation but increased with phosphate limitation. Since our experiments had 25 times more N and P than those of Müller et al., we suggest the changes in the cells size in our treatments were a result of light treatments.

There was a negative log–log trend between chlorophyll *a* concentration per cell and neutral lipids per cell (Fig. 4c) for *Tetraselmis* sp. (log neutral lipids = − 1.29 log chlorophyll a + log 9.24×10^{-3}, $R^2 = 0.69$) and *E. huxleyi*

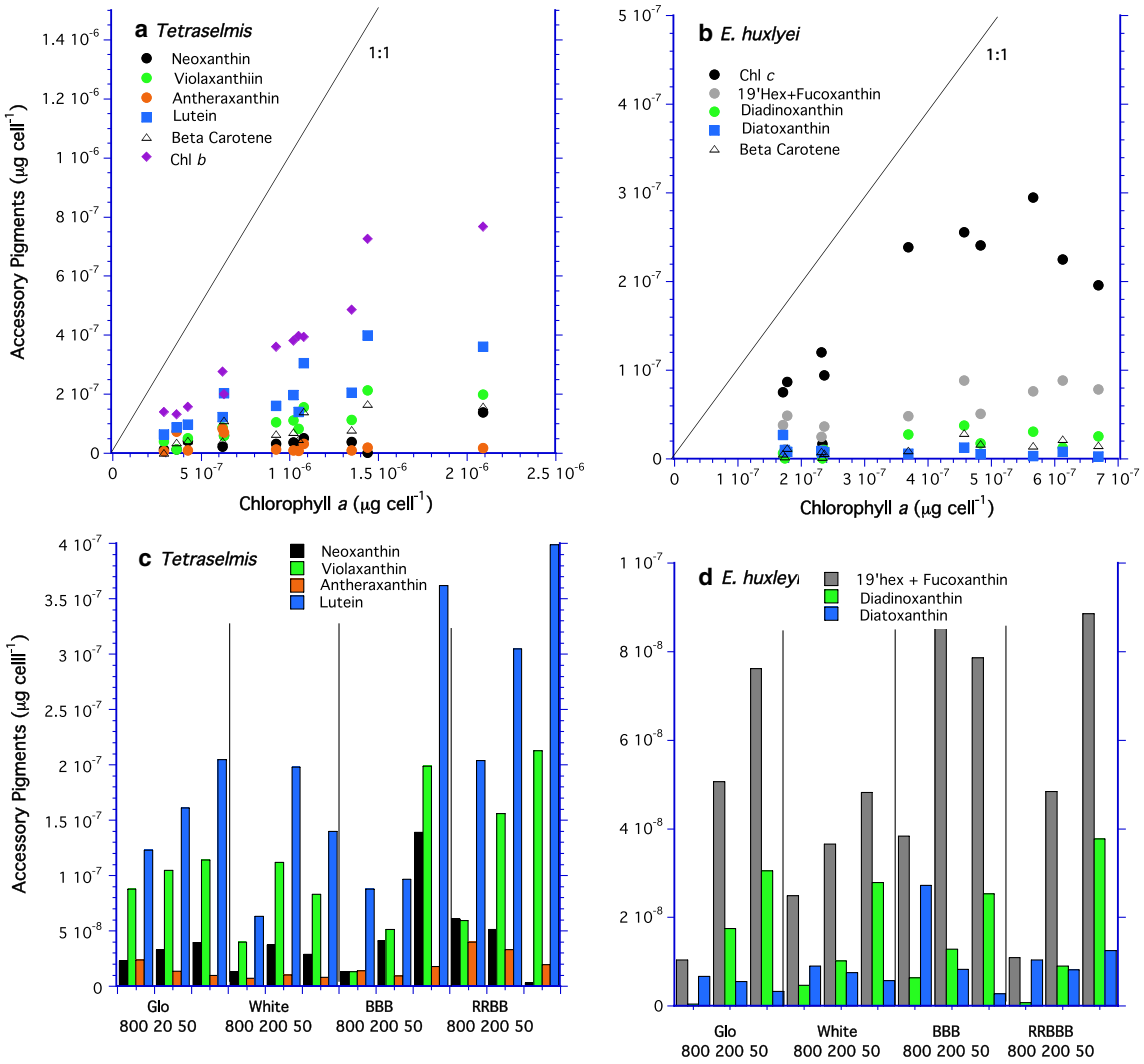

Fig. 5 Accessory pigments. **a** *Tetraselmis* sp. accessory pigments as a function of chlorophyll a, **b** *E. huxleyi* accessory pigments as a function of chlorophyll *a,* **c** *Tetraselmis* sp. accessory pigments as a function of light sources, and **d** *E. huxleyi* accessory pigments as a function of light sources for one sample per treatment

(log neutral lipids = − 0.41 log chlorophyll *a* + log 12,341, $R^2 = 0.60$); however, the slopes were significantly different ($N = 15$, $|t| = 3.02$, $p = 0.005$). When lipid concentrations were normalized by cell volume (Fig. 4d), the slopes for *Tetraselmis* sp. and *E. huxleyi* were only significantly different at the 0.05 level ($R^2 = 0.41$, $N = 15$, $|t| = 2.245$, $p = 0.034$). Although there was considerable scatter in the data, the log slope of − 0.411 showed for every 1000-fold reduction in chlorophyll *a* there was a 2.5-fold increase in neutral lipids.

Increases in chlorophyll *a* concentrations at lower light levels were accompanied by increases in concentrations of certain accessory pigments (Fig. 5a, b). For *Tetraselmis* sp., the accessory pigments lutein and chlorophyll *b* had the highest concentrations and their concentrations increased with chlorophyll *a* levels (Fig. 5a). For *E. huxleyi*, the accessory pigments chlorophyll *c* and fucoxanthins had the highest levels and increased with chlorophyll *a* concentrations (Fig. 5b). Along with lutein, other carotenoids found in *Tetraselmis* sp. cells were beta carotene, neoxanthin, violaxanthin, and antheraxanthin, all in low concentrations. Generally, at high light levels, beta carotene, neoxanthin, and violaxanthin decreased in concentration, while antheraxanthin increased (Fig. 5c). Beta carotene, diadinoxanthin, and diatoxanthin were found in low concentrations in *E. huxleyi,* and the major carotenoid was 19'hexanoyloxyfucoxanthin. The amounts of these carotenoids varied with light levels, where high light caused fucoxanthins, diadinoxanthin, and beta carotene concentrations to decrease and diatoxanthin to increase (Fig. 5d).

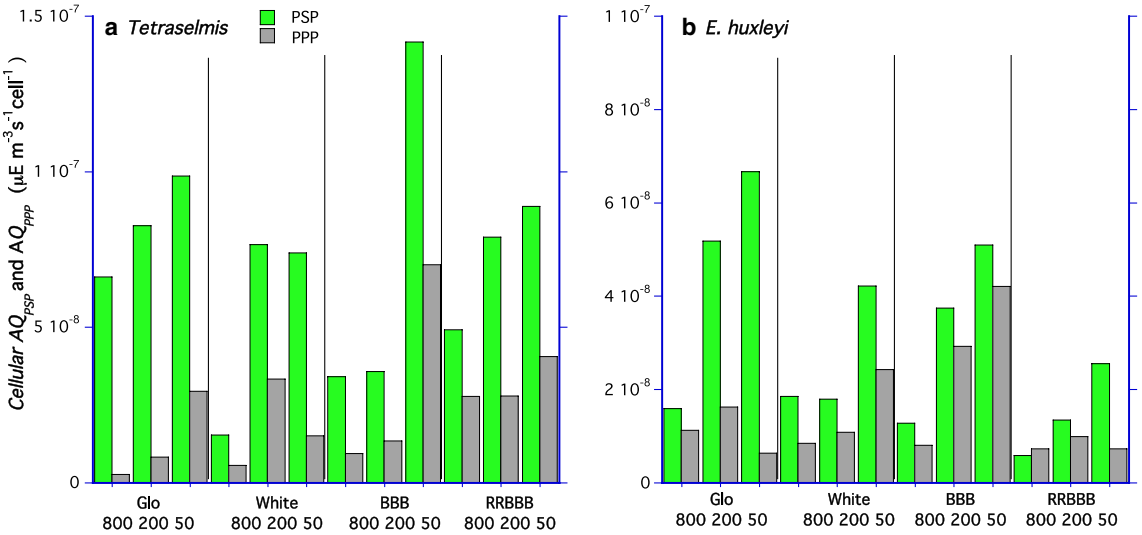

Fig. 6 Quantum light absorption per cell for 3 irradiances levels and the 4 light sources. **a** *Tetraselmis* sp. and **b** *E. huxleyi*, where PSP are photosynthetic pigments and PPP are photoprotective pigments for one sample per treatment

3.3 Bio-optics

The bio-optical effects, on a per cell basis and for total biomass, were accessed for quantum absorption (AQ_{ph}), which is a_{ph}, the sum of the spectrally weighted pigment absorption, multiplied by $Q_{PAR}(\lambda)$, the spectral light intensity of the light source (Eq. 1). On cellular basis, AQ_{PSP} and AQ_{PPP} per cell (i.e., normalized by biomass) increased as light level decreased (Fig. 6a, b); however, this was only significant between the 50 PPFD and 800 PPFD treatments for AQ_{PSP} ($p \le 0.012$) and AQ_{PPP} ($p \le 0.034$). AQ_{PSP} per cell was always higher than AQ_{PPP} per cell, since the photosynthetic pigments were more concentrated in the cells than the PPP xanthophylls. The opposite trend occurred in AQ_{ph}, AQ_{PSP}, and AQ_{PPP} for total quanta absorbed by the biomass. Biomass had the highest total quantum absorption at the highest light levels, and least at the lowest for each light intensity and spectrum (Table 3). For *Tetraselmis* sp., the major absorption was by the PSP system, especially for the three Glo treatments, where AQ_{PSP} absorbed 77–96% of the total quanta. In contrast, AQ_{PPP} only contributed 4–23% (Table 3). For *E. huxleyi,* the percentages of AQ_{PSP} and AQ_{PPP} were quite different and AQ_{PPP} played a more important role, especially for the RRBBB treatment. An ANOVA substantiated a significant difference in AQ_{PSP} versus AQ_{PPP} for *Tetraselmis* sp. ($df = 46$, $|t| = 4.022$, $p < 0.001$). *E. huxleyi,* however, showed no statistical difference in AQ_{PSP} and AQ_{PPP} ($p = 0.689$). Thus, AQ_{PPP} contributed to more photon absorption for *E. huxleyi,* but contributed less to *Tetraselmis* sp. (Table 3). This was substantiated by taking the ratio of AQ_{PPP} to AQ_{PSP}, which was significantly different for the two species ($df = 23$, $F = 7.889$, $p = 0.012$).

Spectral algal absorption per cell, a_{ph}, was higher for *Tetraselmis* sp. (Fig. 7) than for *E. huxleyi* (Fig. 8) given the larger cell size of *Tetraselmis* sp. and thus its larger cross-sectional area. For both species, cell absorption was greatest at 50 PPFD and least at 800 PPFD, which corresponded to the highest pigment concentrations at the lowest light levels and reduced cellular pigment concentrations at the highest light levels (also see Fig. 5). The two highest absorption peaks occurred in the blue wavebands, caused by the combination of chlorophyll and carotenoid pigments while smaller peaks in the orange-red were only a result of chlorophylls *a, b,* and *c*. Nearly 77% of absorption peaks in the blue wavebands of *Tetraselmis* sp. (Fig. 7) were accounted for by photosynthetic pigment concentrations and only 23% by the photoprotective pigment concentrations (i.e., antheraxanthin and beta carotene). These pigment concentrations resulted in 91% of the blue light absorption by a_{PSP} in high light and even higher absorption per cell in low light. *E. huxleyi* followed the same pattern with high absorption in the blue wavebands (Fig. 8), a result of high photosynthetic pigment concentrations, which contributed to 90% of the a_{PSP} absorption per cell. In low light, a_{PPP} for *Tetraslmis* increased as a result of increased beta carotene absorption, even though antheraxanthin decreased when it was epoxidized to violaxanthin. For *E. huxleyi* in low light, a_{PPP} also increased with increasing beta carotene levels, despite the reduction of diatoxanthin, which was converted to diadinoxanthin.

Quantum efficiencies of biomass production were very low for all light sources and intensities with an average of 1.4% for *Tetraselmis* sp. and 1.9% *for E. huxleyi*. The exceptions were for *Tetraselmis* sp. biomass in the Glo 800 PPFD

Table 3 Results of the bio-optical model for total biomass

Treatment	PPFD	AQ^1_{ph}	AQ^1_{PSP}	% Error[2]	ϕ_B	$\phi^3_{B\text{-}PSP}$	ϕ^4_{NL}	$\phi^{3,4}_{NL\text{-}PSP}$
	μE m^{-2} s^{-1}	μE m^{-3} s^{-1}			moles C E^{-1}		Relative	Units
Tetraselmis sp.								
Glo	50	1.01	0.777	22.8	0.005	0.007	0.0021	0.003
	200	4.03	3.64	9.9	0.023	0.026	0.0099	0.011
	800	18.3	17.6	4.1	0.011	0.012	0.0097	0.010
White	50	0.673	0.553	17.8	0.005	0.006	0.0019	0.002
	200	2.14	1.47	31.1	0.029	0.042	0.0141	0.020
	800	2.23	1.61	27.9	0.057	0.080	0.0450	0.062
BBB	50	4.58	2.70	41.0	0.001	0.002	0.0006	0.001
	200	4.79	3.32	30.7	0.004	0.006	0.0029	0.004
	800	4.73	3.51	25.7	0.012	0.016	0.0117	0.016
RRBBB	50	1.35	0.840	37.9	0.005	0.008	0.0022	0.004
	200	6.20	4.32	30.3	0.006	0.008	0.0034	0.005
	800	21.7	12.8	41.2	0.004	0.006	0.0037	0.006
E. huxleyi								
Glo	50	0.537	0.489	8.8	0.037	0.041	0.001	0.001
	200	1.97	1.49	24.2	0.017	0.023	0.001	0.001
	800	42.5	24.7	42.0	0.002	0.003	0.001	0.001
White	50	0.594	0.378	36.3	0.007	0.011	0.000	0.001
	200	0.658	4.13	37.2	0.008	0.012	0.014	0.022
	800	8.74	6.04	30.9	0.016	0.024	0.005	0.007
BBB	50	3.57	1.47	58.8	0.002	0.006	0.000	0.000
	200	2.82	1.23	56.5	0.010	0.024	0.001	0.002
	800	7.84	3.98	49.2	0.008	0.016	0.002	0.004
RRBBB	50	0.336	0.252	25.0	0.042	0.056	0.005	0.007
	200	2.39	1.24	48.3	0.035	0.068	0.004	0.009
	800	5.48	2.04	62.8	0.044	0.119	0.044	0.119

[1] AQ_{ph} and AQ_{PSP} for reconstruction photosynthetic pigment absorption of total biomass

[2] The percent PSP to total pigments, which represents the contribution of PPP pigments

[3] Efficiency calculated without the contribution of PPP

[4] Relative lipid production efficiency derived by normalizing by the maximum lipid fluorescence

treatment with up to 5.8% efficiency and *E. huxleyi* biomass in the RRBBB 800 PPFD treatment with up to 4.4% efficiency. Although photoprotective pigments contribute to overall absorption of light by the cells, they do not directly contribute to the biomass production. Consequently, their contribution was removed by substituting AQ_{PSP} for $AQ_{ph,}$ in Eq. 4. This resulted in high biomass efficiency. The highest biomass efficiency of *E. huxleyi* was for the RRBBB 800 PPFD treatment, which ranged from 5.6 to 11.9%, near the theoretical maximum efficiency of 12.5% Bidigare et al. [3]. For all treatments, except Glo 50 PPFD for *E. huxleyi,* efficiencies for neutral lipid production were highest in the high light regimes. For *Tetraselmis* sp., the highest lipid production efficiency was 4.5% in the white light treatment; however, the efficiency increased to 6.2% when substituting AQ_{PSP} in Eq. 5. Neutral lipid production for *E. huxleyi* was highest in the RRBBB treatment at 4.4%, but increased to 11.9% using AQ_{PSP} to calculate efficiency.

The differences in the antenna pigments of the two species played a major role in the differences in AQ_{ph}, AQ_{PSP}, and AQ_{PPP} for each light regime. Of all the pigments in *Tetraselmis* sp. cells, only beta carotene absorbed highest in the blue blue-green wavelengths (i.e., up to 500 nm). For *E. huxleyi,* all pigments, except for chlorophyll *a*, strongly absorbed into the blue-green band and fucoxanthins even higher, up to 530 nm in the green wavebands. Yet, there were no significant correlations between neutral lipid efficiencies and AQ_{ph}, AQ_{PSP} or AQ_{PPP}, either on a per cell basis or per surface area (not shown). However, when near to saturating light levels (i.e., 200 and 800 PPFD) were compared, the trend in AQ_{PPP} for *E. huxleyi* showed quantum absorption increased with increasing blue light (Fig. 9a) and decreased with increasing blue-green-yellow (Fig. 9b). This trend, however, was not significant for *Tetraselmis* sp., nor were there significant correlations for the percent AQ_{PPP} to the percent red light. Further, there was

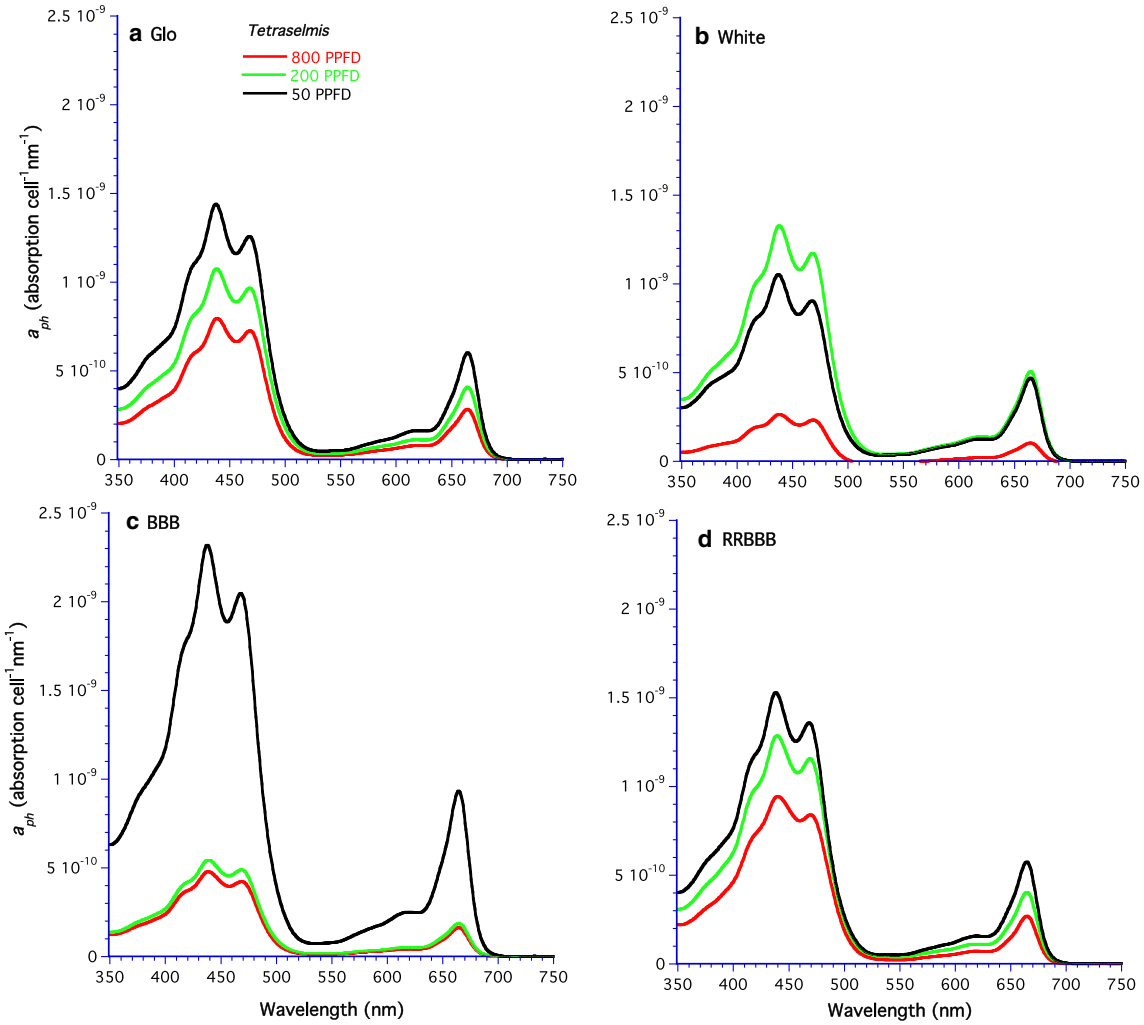

Fig. 7 *Tetraselmis* sp. spectral absorbance per cell, a_{ph}, for the 4 light sources. **a** Glo, **b** white, **c** BBB LEDs, and **d** RRBBB LEDs. a_{ph} was measured by spectrometry and may include pigments other than those in Fig. 5

no correlation of AQ_{PPP} to the ratio of red/blue for either species (Supplement 3a, b).

4 Discussion

4.1 Biomass production

Chromatic adaptation of different species to the light environment has been shown to influence biomass production [7, 42–46]. The higher production rates of *Tetraselmis* sp. in Glo and white light treatments and lower production rate in the BBB light treatment are supported by other studies on green algae [30, 47, 48]. For the *E. huxleyi*, the highest biomass production rate was for the RRBBB treatment, which has been demonstrated for many microalgae rich in blue and blue-green, light absorbing fucoxanthins [19, 20, 28, 46]. The higher biomass production rate of *E. huxleyi* may be the result of photoacclimation to high light and PPP absorption in the blue to blue-green bands, relative to PSP absorption. The fact that the highest production rates for *Tetraselmis* sp. and *E. huxleyi* occurred for spectra having both red and blue wavebands is reminiscent of the Emerson effect for algae, where the maximum photosynthetic rate occurs when red and blue light are combined [19].

4.2 Pigments, neutral lipids, and cell size

Previous studies show low, non-photochemical quenching (NPQ), in cells adapted to high white light (> 1200 PPFD), coincided with the high lipid production [49] and high biomass production [50], which are similar to our finding for *Tetraselmis* sp. Saturating levels of blue light have been shown to produce higher lipid content than white light [22], which was true for our treatments. Further,

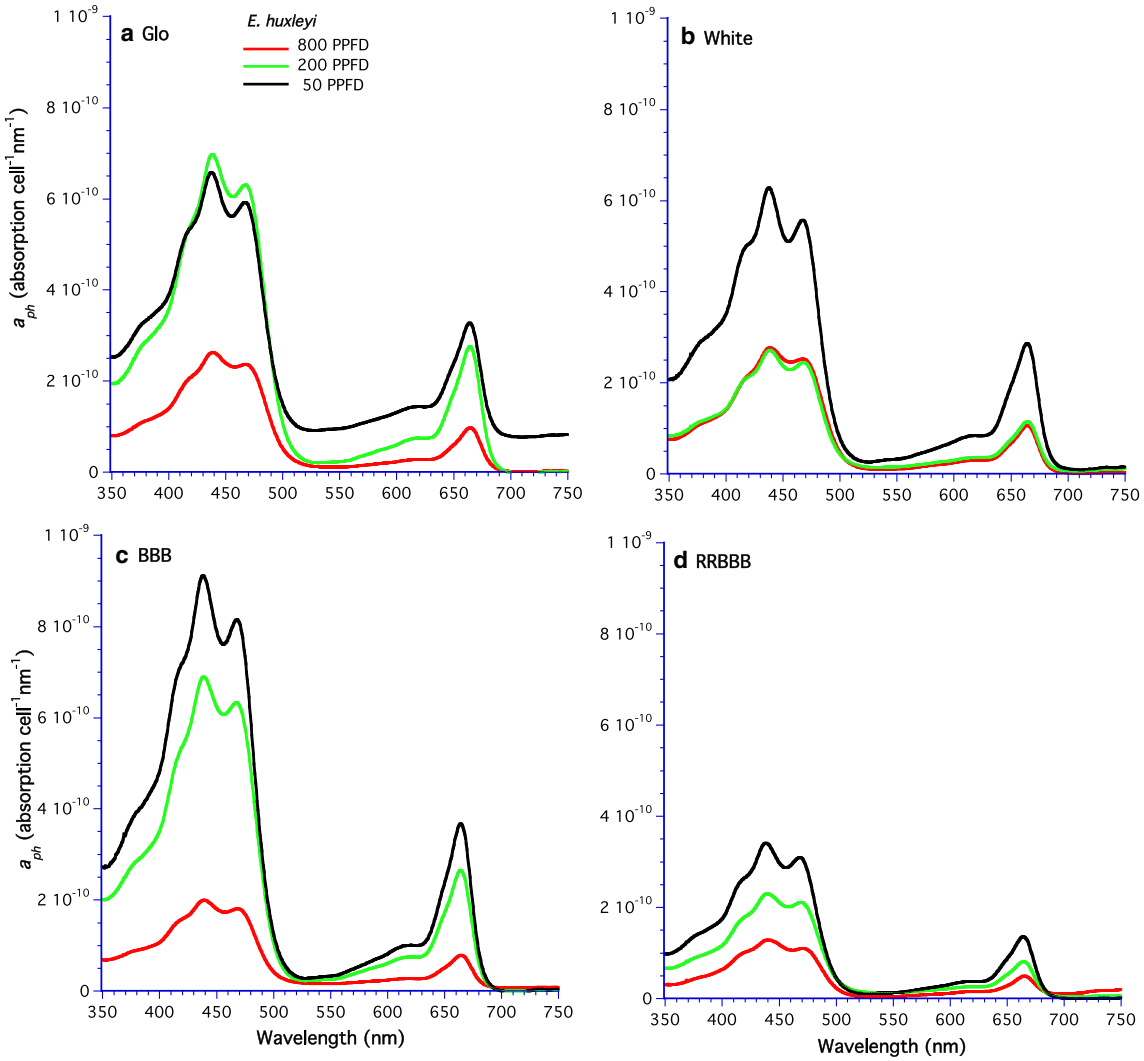

Fig. 8 *E. huxleyi* spectral absorbance per cell, a_{ph}, for 4 light sources. **a** Glo, **b** white, **c** BBB LEDs, and **d** RRBBB LEDs. a_{ph} was measured by spectrometry and may include pigments other than those in Fig. 5

our results support the findings that lipid content is lowest in low light conditions, no matter which spectrum is applied [51, 52]. Low chlorophyll *a* and accessory pigment concentrations at high irradiances are an adaptation by algae to decrease light harvesting pigments in high light environments [53, 54]. Our spectral data support that reaction centers of microalgae, chlorophyll *a* protein complexes, carotenoids, and chlorophylls *b, c* all decrease as light levels increase [55]. In contrast to the chlorophyll *a* trend, high neutral lipid concentrations occurred in high irradiance treatments, which has been also demonstrated by Wu et al. [56]. The 38% increase in *Tetraselmis* sp. cell volume accounted for the near doubling of chlorophyll *a* concentrations in *Tetraselmis* sp. cells and confirmed that larger volumes stored more neutral lipids.

Since lipids are produced in the thylakoid membrane, this may be a physical phenomenon with a trade-off between the volume of lipid droplets produced, the number of reaction centers, and the volume of chloroplasts. Interestingly, neutral lipid globules in stressed microalgae sequester beta carotene and are thought to act as a sunscreen layer [57]. Since lipid bodies are pervasive in many species of microalgae, a high lipid concentration may be an adaptation to light stress.

Photoprotective pigments absorb excess quantum energy that would inhibit the photosystem [58, 59]. Similar to our findings, the increases in photoprotective xanthophylls at high light levels have been attributed to diatoxanthin-diadinoxanthin cycle for *E. huxleyi* [17, 18] and violaxanthin-antheraxanthin-zeaxanthin cycle for green algae [55]. Although no zeaxanthin was detected

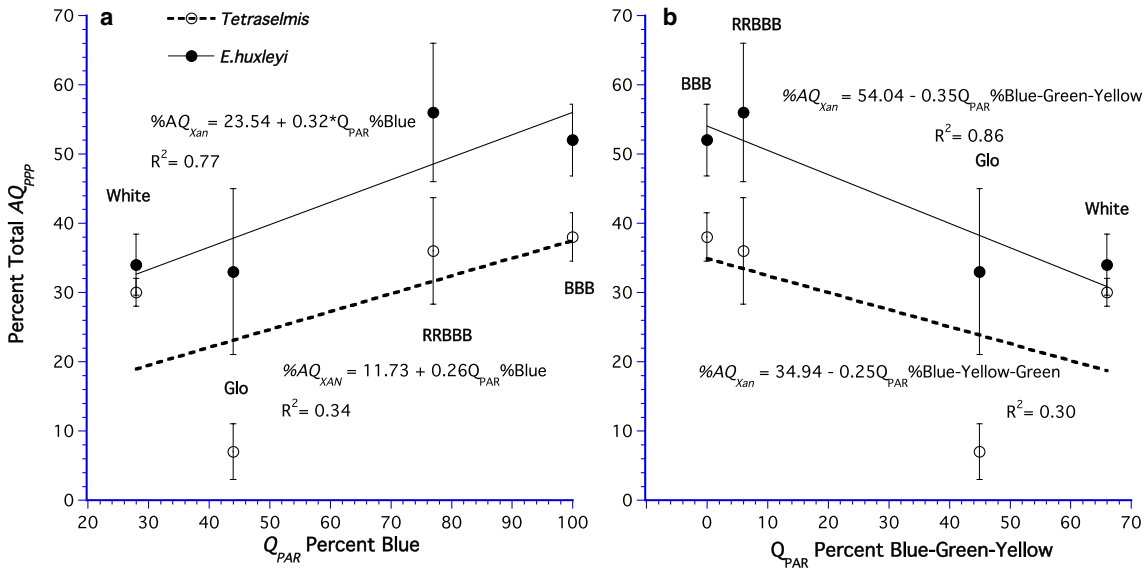

Fig. 9 Percent total quanta absorbed by photoprotective pigments, AQ_{PPP}, for four light sources as a function of: **a** Q_{PAR} percent blue light and **b** Q_{PAR} percent blue-green-yellow light. Means ± 2 standard deviations for each light source ($N = 3$)

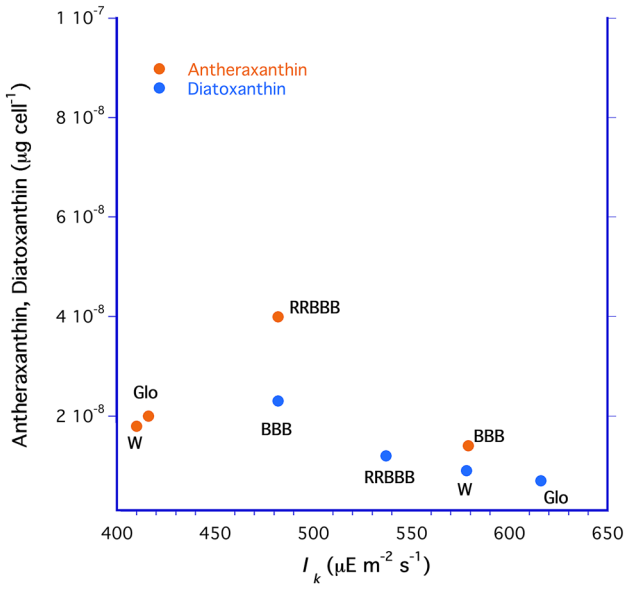

Fig. 10 Concentrations of antheraxanthin and diatoxanthin in the high light treatments as a function of I_k

in *Tetraselmis* sp., violaxanthin (PSP) and antheraxanthin (PPP) were present. Beta carotene also contributed to NPQ and dominated PPP quantum absorption for both species and at most light levels in this study. Beta carotene concentrations increased approximately 50% from high to low light for both *Tetraselmis* sp. and *E. huxleyi*, which compares well with the 33% and 50% increases in beta carotene for *E. huxleyi* measured by Garrido et al. [18] and Mcknew et al. [17], respectively.

4.3 Bio-optics

The uptake of photons by algae was dependent on the specific absorption of the pigments and the concentration of pigments. PPP xanthophylls for the two species have 2.7–3.2 times the specific absorption capacity of chlorophyll *a* [37]. For the PSP light harvesting pigments in *E. huxleyi*, chlorophyll *c* has 4 times higher specific absorption than chlorophyll *a*. In comparison, only lutein (PSP) in *Tetraselmis* sp. has 3 times the specific absorption capacity of chlorophyll *a* [37]. Higher specific absorption is important since, even at low concentrations, pigments can contribute significantly to light absorption in specific wavebands. For example, the high specific absorption of beta carotene is why it dominated PPP absorption over antheraxanthin, even though these pigments had similar concentrations in high light. The dual role of xanthophylls in photoprotection and photosynthesis is regulated by the pH gradient in the thylakoid membrane. De-epoxidization of xanthophylls to photoprotective pigments only occurs if the pH in the thylakoid membrane is below a critical concentration [60]. The strength of the pH gradient depends on the flux of excess irradiance (i.e., above light saturation). However, in this study *Tetraselmis* sp. and *E. huxleyi* treatments saturated at higher light levels and may not have reached the critical pH. This is supported by data in Fig. 10, suggesting I_k may be a good indicator of high light stress and promotion of de-epoxidized xanthophylls.

Larger I_k value indicates a smaller antenna size, which was true for *E. huxleyi*. The linear decrease in I_k with the percent of blue light for *E. huxleyi* (and increase for *Tetraselmis*

sp., *see* Supplement 2b) illustrates a spectral dependence of antenna size. Many studies use short-term photosynthesis measurements of O_2 and ^{14}C, obtaining I_k values that are lower than our values for biomass production. This may be a methodological artifact since the former measurements do not account for higher respiration at lower light levels. High respiration would metabolize more carbon, therefore reducing biomass production and shifting I_k to higher values.

The increase in algal absorption per cell as irradiance decreased was the result of increasing cellular pigment concentrations. This also accounted for the increased quantum absorption per cell as light levels decreased. However, total quantum absorption was higher at higher irradiances as a result of higher biomass and the increased photon flux. Even though cells that adapted to high light had low quantum absorption per cell, more total quanta were absorbed in high light treatments because of their higher biomass. In contrast, low light cells, with high quantum absorption per cell, could not compensate for the lower biomass, and so these treatments always absorbed fewer photons. The consequence for mass cultures, with large volumes and non-homogeneous cell distributions, is that cells trapped in low light dead zones will have lower quantum absorption and production rates than cells in high light regions.

The increased quantum flux of blue light for the LEDs, relative to white and Glo treatments, demonstrates how the unique LED array was tuned to pigment absorption of *E. huxleyi*. Although the percent AQ_{PPP} increased in high light for the LED treatments, the total quanta absorption, AQ_{ph}, remained relatively low, thereby increasing the quantum efficiencies of biomass and neutral lipid production. This was not as evident in *Tetraselmis* sp. cells. The fact that AQ_{PPP} contributed to more photon absorption for *E. huxleyi* and less to *Tetraselmis* sp. corresponds to the highest biomass production rates for *Tetraselmis* sp. in GloPlus and for *E. huxleyi* in RRBBB.

From a practical standpoint, the LED array was a more efficient light source since it generated only the wavelengths that the algae could absorb and did not produce wavelengths that were under-utilized, as did the GloPlus and cool white fluorescent bulbs. This is crucial in cases where biofuel production is augmented by electric lighting since operating expenses and carbon footprints are larger. We estimate the lifetime of our LED array is 5 years (based on a 800 PPFD, 14:10 day/night cycle), more than most efficient cool white and growth fluorescent bulbs of the same intensity. Other advantages of using LEDs tuned to algal action spectra for biofuel bioreactors are that they provide the right mix of spectral irradiance for biomass production, can optimize lipid production, and have lower energy consumption than other commercial light sources.

Our study has confirmed that spectral absorption by algae is a major factor contributing to biomass and lipid production rates for cultures under different light intensities and spectra. By tuning the light spectrum to the absorption spectrum of the algae, both biomass and lipid production can be optimized. Therefore, knowing the spectral properties of microalgae could enhance biofuel production by producing more biomass and lipids, although this will depend on improving photobioreactor designs. Models of photobioreactor mixing that have incorporated scalar irradiance [61–64] and spectral irradiance [65] have shown that continuous mixing in strong light is needed to achieve high biomass production [66]. To enhance biomass and lipid production, the light spectrum could be matched to algal absorption in a well-mixed photobioreactor so that algal cells would experience a high, time-averaged light field with no dead zones to trap cells in suboptimal light levels. Thus, more efficient mixing would reduce extreme highs and lows in light intensities. This, plus the rapid reversibility of PSP to PPP and vise versa, means cells could adjust to light levels without high metabolic costs [8, 67].

5 Conclusions

Spectral quality and intensity of light sources directly influenced the shape of biomass production curves for *Tetraselmis* sp. *and E. huxleyi*. Cells adapted to high irradiance levels had decreased pigment concentrations and spectral absorption per cell, but still exhibited high total quantum absorption as a result of high biomass. High levels of neutral lipids per cell were associated with low, cellular chlorophyll a concentrations. The highest lipid production occurred for *E. huxleyi* under a high red-blue light spectrum using LEDs, even though the LEDs had the same photon flux density as the other light sources.

This study infers that another way to achieve the efficacy of high biomass and lipid production may be to optimize optical properties of the microalgae. This can be accomplished by tuning light sources to pigment distributions in high light regimes, such that cells are not severely photoinhibited or have extreme NPQ. One way to achieve this is to improve mixing conditions in photobioreactors so microalgae adapt to a light regime that, averaged over short timescales, is high and constant.

Acknowledgements We wish to thank Dr. Jeannine Winkler and Christian Rösch for helping with the flow cytometer analyses. The authors are indebted to Daniel Steiner and Blake Mathews at the EAWAG laboratory, Kastanienbaum, Switzerland, for processing the HPLC samples. We also thank Drs. Ulrike Zika and Fabian Ille for proofreading the revised manuscript. Lastly, the comments and suggestions

of three reviewers greatly improved this manuscript and for that, we thank them.

Authors' contributions Dr. Granata designed and conducted experiments and wrote 80% of the manuscript. Drs. Egli, Härri, and Habermacher all contributed the remaining text and optimization of the LED arrays.

Funding This project was funded by a grant to Drs. Granata and Egli from the Office of Research, Hochschule Luzern. Special thanks to Dr. Andrea Weber Marin, vice-dean of the Lucerne School of Engineering and Architecture and Head of Research and Development, for supporting this work.

Compliance with ethical standards

Conflict of interest The authors declare this work has no conflict of interest either personally or financially.

Consent for publication The authors approved the consent for publishing the manuscript.

Data availability Data analyzed in this study are presented in the main manuscript and in supplemental files. Other data files are available in the Lucerne Open Repository (LORY) zenodo.org/communities/lory/.

Ethics approval The authors have read and agreed to the ethics for publishing the manuscript.

References

1. Bidigare R, Smith R, Baker K, Marra J (1987) Oceanic primary production estimates from measurements of spectral irradiance and pigment concentrations. Global Biogeochem Cycles 3:171–186
2. Bidigare R, Ondrusek M, Kiefer D (1990) In-vivo absorption properties of algal pigments. Proc SPIE Intl Soc Opt Eng 1302:290–302
3. Bidigare R, Prezlin B, Smith R (1992) Bio-optical models and problems with scaling. In: Falkowski P, Woodhead A (eds) Primary production and biochemical cycles in the sea. Plenum Press, NY, pp 175–212
4. Smith R, Prézlin B, Bidigare R, Baker K (1989) Bio-optical modeling of photosynthetic production in coastal waters. Limnol Oceanogr 34(8):1524–1544
5. Markager S, Vincent W (2001) Light absorption by phytoplanton: development of a matching parameter for algal photosynthesis under different spectral regimes. J Plankton Res 23(12):1373–1384
6. Kandilian R, Lee E, Pilon L (2013) Radiation and optical properties of Nannochloropsis oculata grown under different irradiances and spectra. Bioresour Technol 137:63–73. https://doi.org/10.1016/j.biortech.2013.03.058
7. Morel A (1998) Optical modeling of the upper ocean in relation to its biogenous matter content (case I waters). J Geophys Res 93:10749–10768
8. Harris G, Scanlan D, Geider R (2009) Responses of *Emiliania huxleyi* (Prymnesiophyceae) to step changes in photon flux density. Eur J Phycol 44(1):31–48. https://doi.org/10.1016/j.biortech.2014.03.092
9. Cullen J, Yang X, McIntyre H (1992) Nutrient limitation and marine photosynthesis. In: Falkowski P, Woodhead A (eds) Primary productivity and biogeochemical cycles in the sea. Plenum Press, NY
10. Kirk J (1992) The nature and measurement of the light environment in the ocean. In: Falkowski P, Woodhead A (eds) Primary productivity and biogeochemical cycles in the sea. Plenum Press, NY, pp 9–29
11. Melis A, Neidhardt J, Benemann J (1999) *Dunaliella salina* (Chlorophyta) with small chlorophyll antenna sizes exhibit higher photosynthetic productivities and photon use efficiencies than normally pigmented cells. J Appl Phycol 10:515–525
12. Nakajima Y, Ueda R (2000) The effect of reducing light-harvesting pigment on marine microalgal productivity. J Appl Phycol 12:285–290
13. Lee J, Mets L, Greenbaum E (2002) Improvement of photosynthetic CO2 fixation at high light intensity through reduction of chlorophyll antenna size. Appl Biochem Biotechnol 98–100:37–48
14. Huesemann M, Hausmann T, Barth R, Akso MM, Weissman J, Benemann J (2009) Biomass productivities in wild type and pigment mutant of *Cyclotella* sp. (Diatom). Appl Biochem Biotechnol 157:507–526. https://doi.org/10.1007/s12010-008-8298-9
15. Perrine Z, Negi S, Sayre R (2012) Optimization of photosynthetic light energy utilization by microalgae. Algal Res 1:134–142. https://doi.org/10.1016/j.algal.2012.07.002
16. Nanninga H, Tyrrell E (1996) Importance of light for the formation of algal blooms by *Emiliania huxleyi*. Mar Ecol Prog Ser 136:195–203
17. Mckew B, Davey P, Finch S, Hopkins J, Lefebvre S, Metodiev M, Oxborough K, Raines C, Lawson T, Geider R (2013) The trade-off between the light-harvesting and photoprotective functions of fucoxanthin-chlorophyll proteins dominates light acclimation in *Emiliania huxleyi* (clone CCMP 1516). New Phytol 200:74–85
18. Garrido J, Brunet C, Rodrĺguez F (2016) Pigment variations in *Emiliania huxleyi* (CCMP370) as a response to changes in light intensity or quality. Environ Microbiol 8(12):4412–4425. https://doi.org/10.1111/1462-2920.13373
19. Schofield O, Bidigare R, Prézelin B (1990) Spectral photosynthesis, quantum yield and blue-green light enhancement of productivity rates in the diatom *Chaetoceros gracile* and the prymnesiophyte *Emiliania huxleyi*. Mar Ecol Prog Ser 64:175–186
20. Marchetti J, Bougaran G, Jauffrais T, Lefebvre S, Rouxel C, Saint-Jean B, Lukomska E, Robert R, Cadoret J (2013) Effects of blue light on the biochemical composition and photosynthetic activity of *Isochrysis* sp. (T-iso). J Appl Phycol 25(1):109–119
21. Jeon Y-C, Cho C-W, Yun Y-S (2005) Measurement of microalgal photosynthetic activity depending on light intensity and quality. Biochem Eng J 27:127–131
22. Atta M, Idris A, Bukhari A, Wahidin S (2013) Intensity of blue LED light: a potential stimulus for biomass and lipid content in fresh water microalgae *Chlorella vulgaris*. Bioresour Technol 148:373–378. https://doi.org/10.1016/j.biortech.2013.08.162
23. Pérez-Pazos J-V, Fernández-Izquierdo P (2011) Synthesis of neutral lipids in *Chlorella* sp. under different light and carbonate conditions. CT&F-Ciencia Technologia y Futura 4(4):47–57
24. Ra C, Kang C-H, Jung J-H, Jeong G-T, Kim S-K (2016) Effects of light-emitting diodes (LEDs) on the accumulation of lipid content using a two-phase culture process with three microalgae. Bioresour Technol 212:254–261. https://doi.org/10.1016/j.biortech.2016.04.059
25. Wang C-Y, Fu C-C, Liu Y-C (2007) Effects of using light-emitting diodes on the cultivation of *Spirulina platensis*. Biochem Eng J 37:21–25. https://doi.org/10.1016/j.bej.2007.03.004
26. Bland E, Angenent L (2016) Pigment-targeted light wavelength and intensity promotes efficient photoautotrophic growth of

Cyanobacteria. Bioresour Technol 216:579–586. https://doi.org/10.1016/j.biortech.2016.05.116
27. Molina Grima E, García Camacho F, Sánchez Pérez J, Contreras Gómez A, Valdés Sanz F (1994) Outdoor turbidostat culture of the marine microalga *Tetraselmis* sp. Aquacult Res 25(5):547–555. https://doi.org/10.1111/j.1365-2109.1994.tb00718.x
28. Aidar E, Gianesella-Galvão S, Sigaud T, Asano C, Liang T, Rezende K, Oishi M, Aranha F, Milani G, Sandes M (1994) Effects of light quality on growth, biochemical composition and photosynthetic production in *Cyclotella caspia* Grunow and *Tetraselmis gracilis* (Kylin) Butcher. J Exp Mar Biol Ecol 180(2):175–187
29. Go S, Lee S-J, Jeong G-T, Kim S-K (2012) Factors affecting the growth and the oil accumulation of marine microalgae, *Tetraselmis suecica*. Bioprocess Biosyst Eng 35:145–150. https://doi.org/10.1007/s00449-011-0635-7
30. Abiusi F, Sampietro G, Marturano G, Biondi N, Rodolfi L, D'Ottavio M, Tredici M (2013) Growth, photosynthetic efficiency, and biochemical composition of *Tetraselmis suecica* F&M-M33 grown with LEDs of different colors. Biotechnol Bioeng 111(5):956–964. https://doi.org/10.1002/bit.25014
31. Xu D, Gao Z, Li F, Fan X, Zhang X, Ye N, Mou S, Liang C, Li D (2013) Detection and quantitation of lipid in the microalga *Tetraselmis subcordiformis* (Wille) Butcher with BODIPY 505/515 staining. Bioresour Technol 127:386–390
32. Guillard R (1975) Culture of phytoplankton for feeding marine invertebrates. In: Smith W, Chanley M (eds) Culture of marine invertebrate animals. Plenum Press, NY, pp 26–60
33. Pretet P, Reynaud S, Ferrier-Pagès C, Gattuso J-P, Kamber B, Samankassou E (2014) Effect of salinity on the skeletal chemistry of cultured scleractinian corals: Cd/Ca ratio as a potential proxy for salinity reconstruction. Coral Reefs 33:169–180
34. Guzman H, del la Jara Valdido A, Carmona Duarte L, Freijanes Presmanes L (2010) Estimate by means of flow cytometry of variation in composition of fatty acids from *Tetraselmis suecica* in response to culture conditions. Aquacult Intl 8:189–199. https://doi.org/10.1007/s10499-008-9235-1
35. Van Wychen S, Ramirez S, Laurens L (2015) Determination of total lipids as fatty acid methyl esters (FAME) by in situ transesterification. Technical Report NREL/TP-5100-60958 12
36. SCOR-UNESCO (1996) Determination of photosynthetic pigments in sea-water. Monographs onoceanographic methodology 1. Unesco, Paris, pp 1–66
37. Thrane J-E, Kyle M, Striebel M, Haande S, Grung M, Rohrlack T, Andersen T (2015) Spectrophotometric analysis of pigments: a critical assessment of a high-throughput method for analysis of algal pigment mixtures by spectral deconvolution. PLoS ONE 10(9):e0137645. https://doi.org/10.1371/journal.pone.0137645
38. Stucki R (2012) Spectral LED light. Lucerne University of Applied Sciences and Arts, Lucerne
39. Latowski D, Kuczyńska P, Strzałka K (2011) Xanthophyll cycle – a mechanism protecting plants against oxidative stress. Redox Rep 16(2):78–90. https://doi.org/10.1179/174329211X13020951739938
40. Platt T, Jassby A (1976) The relationship between photosynthesis and light for natural assemblages of coastal marine phytoplankton. J Phycol 12:421–430. https://doi.org/10.1111/j.1529-8817.1976.tb02866.x
41. Müller M, Anita A, LaRoche J (2008) Influence of cell cycle phase on calcification in the coccolithophore *Emiliania huxleyi*. Limnol Oceanogr 53(2):506–512
42. Wang C-Y, Fu C-C, Liu Y-C (2007) Effects of using light-emitting diodes on the cultivation of *Spirulina platensis*. Biochem Eng J 37:21–25
43. Carvalho A, Silva S, Baptista J, Malcata F (2011) Light requirements in microalgal photobioreactors - an overview of aspects. Appl Microbiol Biotechnol 89:1275–1288
44. Hultberg M, Jönsson H, Bergstrand K-J, Carlsson A (2014) Impact of light quality on biomass production and fatty acid content in the microalga *Chlorella vulgaris*. Bioresour Technol 159:465–467. https://doi.org/10.1016/j.biortech.2014.03.092
45. Teo C, Atta M, Bukhari A, Taisir M, Yusuf A, Idus A (2014) Enhancing growth and lipid production of marine microalgae for biodiesel production via the use of different LED wavelengths. Bioresour Technol 162:38–44. https://doi.org/10.1016/j.biortech.2014.03.113
46. Sánchez-Saavedra M, Maeda-Martínez A, Acosta-Galindo S (2016) Effect of different light spectra on the growth and biochemical composition of *Tisochrysis lutea*. J Appl Phycol 28:839–847. https://doi.org/10.1007/s10811-015-0656-8
47. Baba M, Kikuta F, Suzuki I, Watanabe M, Shiraiwa Y (2012) Wavelength specificity of growth, photosynthesis, and hydrocarbon production in the oil-producing green alga *Botryococcus braunii*. Bioresour Technol 109:266–270
48. Vidiveloo A, Moheimani N, Cosgrove J, Bahri P, Parlevliet D (2015) Effect of different light spectra on the growth and productivity of acclimated *Nannochloropsis* sp. (Eustigmatophyceae). Algal Res 8:121–127. https://doi.org/10.1016/j.algal.2015.02.001
49. Simionato D, Sforza E, Carpinelli E, Bertucco A, Giacometti G, Morosinotto T (2011) Acclimation of *Nannochloropsis gaditana* to different illumination regimes: effects on lipids accumulation. Bioresour Technol 102:6026–6032. https://doi.org/10.1016/j.biortech.2011.02.100
50. Berteotti S, Ballottarim M, Bassi R (2016) Increased biomass productivity in green algae by tuning nonphotochemical quenching. Sci Rep 6:21339. https://doi.org/10.1038/srep21339
51. Chen Y, Vaidyanathan S (2013) Simultaneous assay of pigments carbohydrates proteins and lipids in microalgae. Anal Chim Acta 776:31–40. https://doi.org/10.1016/j.aca.2013.03.005
52. Seo Y, Cho C, Lee J-Y, Han J-I (2014) Enhancement of growth and lipid production from microalgae using fluorescent paint under the solar radiation. Bioresour Technol 173:193–197. https://doi.org/10.1016/j.biortech.2014.09.012
53. Prézelin B (1981) Light reactions in photosynthesis. In: Platt T (ed) Physiological bases of phytoplankton ecology. Canadian bulletin of fisheries and aquatic sciences, pp 1–43
54. Falkowski P (1992) Molecular ecology of phytoplankton physiological. In: Falkowski P, Woodhead A (eds) Primary production and biochemical cycles in the sea. Plenum Press, NY, pp 47–67
55. Bonente G, Pippa S, Castellano S, Bassi R, Ballotari M (2012) Acclimation of *Chlamydomonas reinhardtii* to different growth irradiances. J Biol Chem 287(8):5833–5847
56. Wu Y-H, Yu Y, Hu H-Y (2014) Effects of initial phosphorus concentration and light intensity on biomass yield per phosphorus and lipid accumulation of *Scenedesmus sp* LX1. Bioenerg Res 7:927–934. https://doi.org/10.1007/s12155-014-9411-2
57. Varela J, Pereira H, Vila M, León R (2015) Production of carotenoids by microalgae: achievements and challenges. Photosynth Res 125(3):423–436. https://doi.org/10.1007/s11120-015-0149-2
58. Niyogi K, Shih C, Chow W-S, Pogson B, DellaPenna D, Björkman O (2001) Photoprotection in a zeaxanthin- and lutein-deficient double mutant of *Arabidopsis*. Photosynth Res 67:139–145
59. Jahns P, Hoolwarth A (2012) The role of the xanthophyll cycle and of lutein in photoprotection of photosystem II. Biochim Biophys Acta 1817:182–193. https://doi.org/10.1016/j.bbabio.2011.04.012
60. Mewes H, Richter M (2002) Supplementary ultraviolet-b radiation induces a rapid reversal of the diadinoxanthin cycle in the strong light-exposed diatom *Phaeodactylum tricornutum*. Plant Physiol 130:1527–1535
61. Molina Grima E, García Camacho F, Sánchez Perez J, Fernández Sevilla J, Acién Fernández F, Contreras Gómez A (1994) A mathematical model of microalgal growth in light-limited

chemostat culture. J Chem Tech Biotechnol 61:67–173. https://doi.org/10.1002/jctb.280610212
62. Zijffers J-W, Schippers K, Zheng K, Janssen M (2010) Maximum photosynthetic yield of green microalgae in photobioreactors. Mar Biotechnol 12:708–718. https://doi.org/10.1007/s10126-010-9258-2
63. Huesemann M, Crowe B, Waller P, Chavis A, Hobbs S, Edmundson S, Wigmosta M (2016) A validated model to predict microalgae growth in outdoor pond cultures subjected to fluctuating light intensities and water temperatures. Algal Res 13:195–206. https://doi.org/10.1016/j.algal.2015.11.008
64. Qin C, Lei Y, Wu J (2018) Light/dark cycle enhancement and energy consumption of tubular microalgal photobioreactors with discrete double inclined ribs. Bioresour Bioprocess 5:28. https://doi.org/10.1186/s40643-018-0214-8
65. Niizawa I, Heinrich J, Irazoqui H (2014) Modeling of the influence of light quality on the growth of microalgae in a laboratory scale photo-bio-reactor irradiated by arrangements of blue and red LEDs. Biochem Eng J 90:214–223. https://doi.org/10.1016/j.bej.2014.05.002
66. Richmond A, Cheng-Wu Z, Zarmi Y (2003) Efficient use of strong light for high photosynthetic productivity - interrelationships between the optical path, the optimal population density and cell-growth inhibition. Biomol Eng 20(4–6):229–236
67. Van de Poll W, Buma A (2009) Does ultraviolet radiation affect the xanthophyll cycle in marine phytoplankton? Photochem Photobiol Sci 8:1295–1301. https://doi.org/10.1039/B904501E